On the Interaction between the Ion Cyclotron Resonance Heating and Scrape-off Layer Turbulence *via* Coherent Waves

G. Antar[1], M. Goniche[2], A. Ekedahl[2] and L. Colas[2]

[1] *American University of Beirut, Riad el-Solh, Beirut 1107-2020, Lebanon*

[2] *CEA, IRFM, F-13108 Saint-Paul-lez-Durance, France*

Introduction Wave heating is launched by antennas installed inside the vacuum chamber emitting at particular frequencies known to be absorbed by the plasma. It was shown that transport in the SOL is caused by incoherent eddies leading to 'diffusive transport' and by convective large-scale structures called avaloids [1] leading to 'convective transport' with similar properties recorded on various magnetic fusion devices [2]. Morisaki *et al.* on the compact helical system were the first to report turbulence decrease in the presence of ICRH outside the last closed flux surface (LCFS) with a threshold of 300 kW [3]. In Ref. [4], the effects of ICRH on turbulence in-between ELMs and on the ELM-induced transport was studied on the ASDEX-Upgrade tokamak where it was reported that turbulence intermittent bursts in the SOL were suppressed leading to Gaussian distribution functions of the density fluctuations and a strong modification of their power spectra. The effect of ICRH on ELMs was observed to be important with a reduction of a factor of three in the induced transport with respect to only NBI-driven H-mode plasmas. These results were confirmed on the Tore Supra tokamak [5].

The Experimental Setup The experiments presented here were conducted on the Tore Supra tokamak. The two Langmuir probes used here have a diameter of 5 mm and toroidally separated by 1 cm. The closed magnetic field lines in front of the probe are marginally connected to the bottom of the ICRH antenna Q1 and the top of antenna Q5 and they are far from antenna Q2 (see Ref. [5]). The tips are not in direct interaction with the RF field but could detect the effects of ICRH as the plasma is transported radially outward towards into the SOL form the edge. A constant -100 V bias is applied leading to signals reflecting the ion saturation current (I_{sat}) which are acquired by two diagnostics: DCEDRE, where the acquisition frequency is 200 MHz with 200,000 points per trigger and per channel. A high-pass analog filter cuts off the fluctuation below 100 kHz. Simultaneously, and using the same trigger, data are also recorded on DFLUC at a rate of 1 MHz, with 13,600 points per trigger per channel.

The Power Spectra The power spectra, defined as $S_f(I) = \langle|\tilde{I}(f)|^2\rangle$ where $I = I_{sat} - \langle I_{sat}\rangle$ are plotted around the source frequencies of the Q1, Q5 and Q2 antennas in Fig. 1. In Fig. 1, the frequency spectra of I using the DCEDRE is shown for the frequency range $0.1 > f >$ 10 MHz. The spectrum of the ohmic plasma decreases with increasing frequency until about

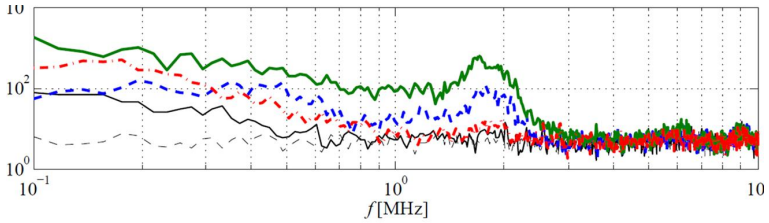

Figure 1: The power spectra with $0.1 > f > 10$ MHz is shown (from DCEDRE). The dashed line represents instrumental noise, in dotted ohmic plasma and in thick solid, thick dashed and thick dash-dotted the cases when Q1, Q5 and Q2 antennas are active respectively.

700 kHz. When Q2 is active, the total level of fluctuations increases with the average edge density, nevertheless, only one scaling region is detected similar to the ohmic plasma case. A small intensity peak is detected about $f_s = 1.7$ MHz which appears to be the same for the three antennas but its amplitude is quite different for Q1, Q5 and Q2.

The Cross-correlation The two probes, apart toroidally by $d = 1$ cm, are used to calculate the cross-correlation coefficient. Fig. 2(a) illustrates $C_{12}(\tau)$ for ohmic plasma and when Q1 and Q5 are active. The first striking feature is the existence of a damped oscillation reflecting contributions at low frequencies and another at high frequencies. In order to emphasize the contribution of the peak at 1.7 MHz, we filter the signals around this value and determine $C_{12}(\tau)$.

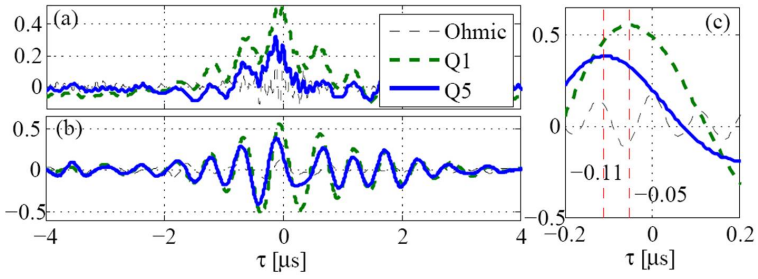

Figure 2: (a), the cross-correlation coefficient as a function of time is plotted for the ohmic case and when Q1 and Q5 are active. (b), *idem* as in (a) but the data is filtered with a band-pass filter centered around 1.7 MHz. In (c), we zoom on the cross-correlation coefficient in order to emphasize its maximum is shifted towards negative times illustrated by the vertical dashed line.

The result is shown in Fig. 2(b) where the wave structure is clear. In the sub-plot of Fig. 2(c), we zoom on C_{12} to show that the time delay between the two signals is $\tau_0 \simeq 0.8 - 1.2 \times 10^{-7}$ s leading to an average toroidal velocity $U_0 = d/\tau_0 \simeq 0.8 - 2 \times 10^5$ m/s. With the speed and the frequency experimentally determined, we obtain the wavelength $\lambda_s = U_0/f_s \simeq 5 - 11$ cm. The only plasma characteristic velocity of this order ($\sim 10^5$ m/s) is the ion sound speed,

$c_s \simeq 10^3\sqrt{T_e}$. If $c_s = U_0$, then the electron temperature should be $T_e \sim 100$ eV which is typical to the plasma edge. On the other hand, the estimated wavelength, $(5-11)$ cm, is in good agreement with the theory according to which the excitation of sound waves is expected following a parametric decay instability (PDI) [6]. The source of this instability is the temperature anisotropy achieved, for example, by minority heating. In Ref. [6] the sound wavelength was even determined to be about 6-10 cm for tokamak conditions which is close the value obtained experimentally here.

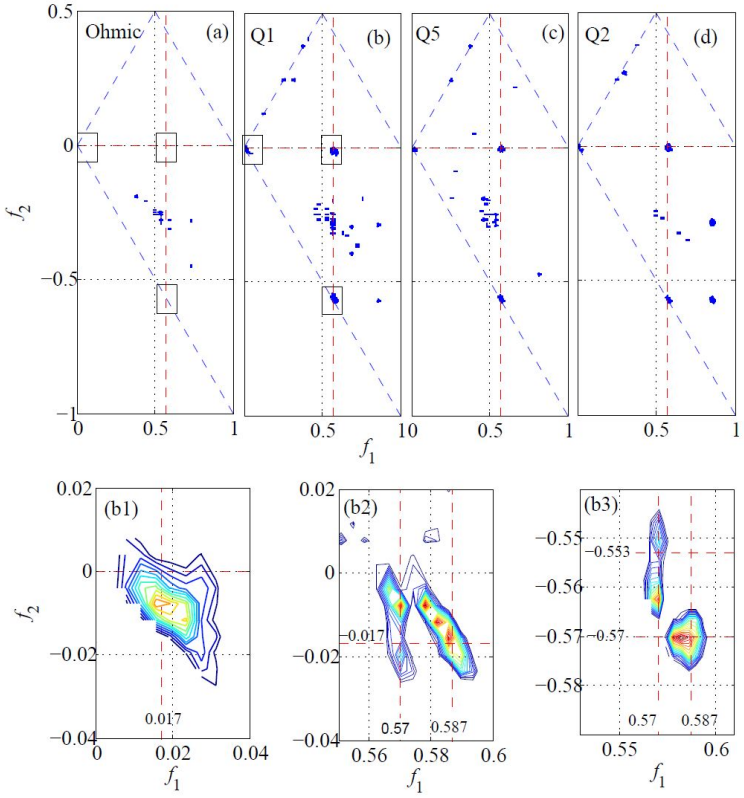

Figure 3: (a)-(d) show the contour plots of γ for ohmic plasma and heated using respectively Q1, Q5 and Q2 as a function of the normalized frequencies f_1 and f_2. In (a) and (b), three squares are inserted in order to show the strong difference between with and without ICRH. The zooms are plotted in (b1), (b2) and (b3) emphasizing that the sound wave at 0.017 is generated by the ICRH and that it is nonlinearly coupled to turbulence. The spots observed outside these squares are mainly caused by instrumental noise.

The Bicoherence The non-linear interaction between the different parts of the spectrum is revealed using the bispectral analysis [7, 8, 9]. The bicoherence γ takes values different from zero in the (f_1, f_2)-plane at frequencies f_1 and f_2 only if there exist a third signal with frequency f such that $f = f_1 \pm f_2$ reflecting the fact that f_1 and f_2 are nonlinearly coupled to form f. Fig. 3(a)-(d) respectively show the contour plots of γ with ohmic heating and with Q1, Q2 and

Q5 respectively active as a function of f_1 and f_2; The frequencies are normalized to the Nyquist frequency here equals to 100 MHz. The contour plots suggest major modifications of the bicoherence when ICRH is turned on mainly at the three following crossings ($f_1 \simeq 0, f_2 \simeq 0$), ($f_1 \simeq 0, f_2 \simeq -0.57$) and ($f_1 \simeq 0.57, f_2 \simeq -0.57$). For ohmic plasma, there exist some spikes in (a) but one can rapidly verify that they have low amplitudes when compared to the case with ICRH. The zoom on the crossing ($f_1 \simeq 0.57, f_2 \simeq -0.57$) in Fig. 3(b) is shown in (b3). Two peaks appear clearly at ($f_1 = 0.57, f_2 \simeq -0.553$) and ($f_1 \simeq 0.587, f_2 \simeq -0.57$). This reflects strong bicoherence caused by the PDI of the ICRH pump decaying into a wave at 1.7 MHz, in the range of ion sound waves and the excitation of the wave at f_2. In this subplot, we just demonstrated the existence of the PDI by using the bicoherence which lead to the identification of f_2 something we were not able to do using the auto-power spectrum. The zoom on the crossing ($f_1 \simeq 0.57, f_2 \simeq -0.017$) is shown in (b2) reflecting also that the sound wave at 1.7 MHz is nonlinearly coupled to 0.587 in agreement with the result in (b1). Lastly, we zoom on the bicoherence spectrum at frequencies around 0 and the result is shown in (b1) which indicates a coupling between $f_1 = 0.017$, which could be linked to ion sound waves, and lower frequencies which reflects turbulence. Accordingly, the oscillations at 1.7 MHz are coupled to turbulence *via* the three-wave coupling; this coupling is simply non-existent without ICRH.

Conclusion We have experimentally shown that the ICRH wave undergoes a parametric decay instability generating waves about 1.7 MHz in the range of the ion sound waves with a wavelength of 5-11 cm. Using bispectral analysis two main conclusions are obtained: (1), the wave at 1.7 MHz frequency is generated from the ICRH (57 MHz) by PDI; (2), the waves at 1.7 MHz are nonlinearly coupled to lower frequencies turbulent fluctuations which is an indication that the coherent oscillation may play an important role in the modification of turbulence in the SOL.

References

[1] G. Y. Antar, *et al. Phys. Rev. Lett.*, 87:065001, 2001.

[2] G. Antar, G. Counsell, Y. Yu, B. LaBombard, and P. Devynck. *Phys. Plasmas*, 10:419, 2003.

[3] T Morisaki, *et al. Plasma Phys. Control. Fusion*, 37:787, 1995.

[4] G. Antar, *et al. Phys. Rev. Lett.*, 105:165001, Oct 2010.

[5] G. Antar, M. Goniche, A. Ekedahl, and L. Colas. *Nuclear Fusion*, 52(10):103005, 2012.

[6] R. M. Galvao, G. Gnavi, L. Gomberoff, and F. T. Gratton. *Plasma Phys. Control. Fusion*, 36:1679-1689, 1994.

[7] Ch.P. Ritz and E. J. Powers. *Physica*, 20D:320–334, 1986.

[8] Ch. P. Ritz, E. J. Powers, , and R. D. Bengtson. *Phys. Fluids B*, 1:153–163, 1989.

[9] B. Ph. Van Milligen, C. Hidalgo, and E. Sanchez. *Phys. Rev. Lett.*, 74:395, 1995.